SYMPOSIUM ON SIMULATION IN ARCHITECTURE + URBAN DESIGN
SimAUD 2020

Predicting Space Usage by Multi-Objective Assessment of Outdoor Thermal Comfort around a University Campus

Patrick Kastner[1], **Timur Dogan**[1]

[1]Environmental Systems Lab, Cornell University, Ithaca, NY, USA, pk373@cornell.edu

ABSTRACT

With the impending issues regarding global warming, urban design is considered a key driver to improve the microclimate in cities. For public spaces, studies suggest that outdoor thermal comfort may be seen as a proxy for space usage in turn attractiveness to people. Although the topic has gained interest in recent years, the discussion so far has focused on computing the metrics rather than deriving interventions from them. Here, we use the tool Eddy3D to model and analyze the outdoor thermal comfort of a designated area around a university campus. Further, we demonstrate how to estimate space usage from those results. Finally, we conduct a spatial sensitivity analysis of the underlying results as a step towards decision aiding. Our work demonstrates how decision-makers may derive areas where interventions will likely have the largest impact on outdoor thermal comfort performance.

Author Keywords

Outdoor Thermal Comfort, Sensitivity Analysis, CFD, MRT, Space Usage

1 INTRODUCTION

Climate change scenarios suggest disconcerting outcomes for the future of cities, especially in urbanized and dense locations. As a result of changing urban microclimates, there is not only increased competition over the wind, sun, and daylight [6], but also a growing risk for detrimental impacts on aspects of the city life; public health, commercial activities, active mobility, and space usage among them [17]. However, the fact that urban microclimates are shaped by the way cities are built also opens new opportunities. For these reasons, the prediction of outdoor thermal comfort has become an increasingly relevant area of research.

In the early 1980s, Whyte [19] devoted a significant amount of time to studying how people use public spaces in US cities, and why some plazas show different usage patterns than others. From video recordings, they counted the number of dwellers which revealed that access to sunlight can be a major factor for plaza use. For NYC, they found that there is a strong correlation between space usage and exposure to sunlight while in other months the microclimate was less relevant. Direct exposure to sunlight is preferred through May during which time the ambient temperature has yet reached comfortable levels. By contrast, in months from June through August, people show little preference between sun and shade and other social parameters and amenities were determining factors [18].

This study frames simulated-based microclimate assessment as a multiple-criteria evaluation problem. It aims to assess the microclimate conditions on a university campus from which outdoor space use, a proxy for the attractiveness of outdoor spaces, is derived. This is motivated by the fact that the majority of the student population is on campus during spring and fall when outdoor thermal comfort is highly dependent on sun and wind exposure. The framework of this analysis is justified with a two-at-a-time and a global sensitivity analysis. The spatial sensitivity adds a layer to the results that allow decision-makers to deduce where geometric interventions will likely have the largest impact on the performance.

2 METHODOLOGY

This study utilizes a simulation tool called Eddy3D to simulate the annual outdoor thermal comfort around an existing building arrangement on the Cornell University campus. The weather data for this study were retrieved from the EnergyPlus repository by the Department of Energy[1] and classifies as warm-summer humid continental climate (Dfb) according to the Köppen classification.

2.1 Case study: Engineering Quad at Cornell University

The CAD model used is comprised of Cornell's Engineering Quad in Ithaca, upstate NY, see Figure 1. As the elevation differences between the buildings are insignificant, they have been neglected in the CAD model.

2.2 Universal Thermal Climate Index (UTCI)

Like other outdoor comfort metrics, the UTCI was developed as an equivalent temperature measure. It is based on a multi-node thermo-physical model that was coupled with an adaptive clothing model [8]. Thus, for any combination of air temperature, wind, radiation, and humidity, the UTCI is defined as the air temperature of a particular reference condition which would cause the same thermal sensation as predicted by the model [5]. We chose the UTCI as a metric, as several studies have shown the UTCI to be a suitable metric that is sensitive and accurate for cold temperatures while also achieving good

[1] Syracuse-Hancock.Intl.AP.725190_TMY3

SimAUD 2020 May 25-27, Online

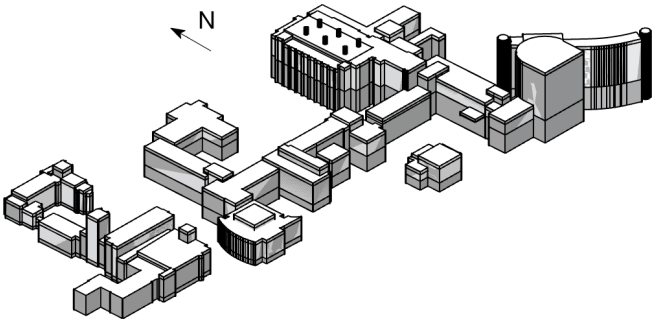

Figure 1. CAD model of the Cornell University engineering quad.

agreement with human responses in tropical climates [14]. Mathematically, the UTCI is computed with a polynomial approximation of four input variables:

$$UTCI = T_{amb} + f(T_{amb}, T_{MRT}, U_{Wind}, p_{vapour}) \quad (1)$$

where T_{amb} is the ambient temperature, T_{MRT} is the mean radiant temperature, U_{Wind} is the wind velocity, and p_{vapour} refers to the vapor pressure, which is a function of the dry-bulb temperature. The resulting UTCI temperatures may be classified and reported as thermal stress categories ranging from "extreme cold stress" to "extreme heat stress". Ideally, one would strive for maximizing the annual urban climate for the "No thermal stress" condition, which falls in the range of 9°C and 26°C.

Empirical data that has been collected by Reinhart et al. [15], confirmed studies undertaken by White. Over one year, the number of people with WiFi devices in a public courtyard on a university campus has been recorded. It has been shown that people take longer lunch breaks when in "no thermal stress" conditions. This suggests that people prefer being in outdoor spaces if the microclimatic conditions are within the "no thermal stress" category. Their findings are summarized in Figure 2.

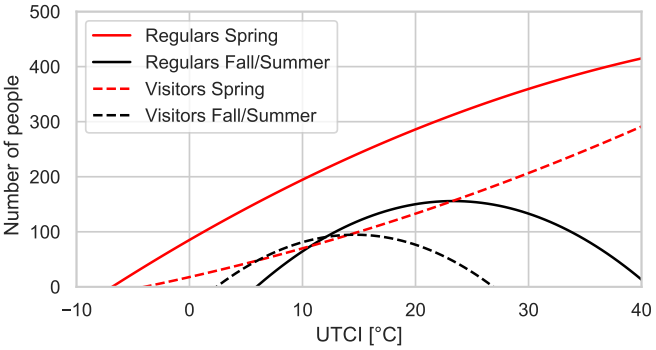

Figure 2. Collocation of empirical outdoor thermal comfort and space usage correlations collected by Reinhart et al.

2.3 Sensitivity analysis

To identify the dominant input parameters of the UTCI metric in this particular temperate climate, and to deduce actionable suggestions on how the microclimate could be improved, sensitivity analyses were carried out in three stages. First, a two-at-a-time sensitivity analysis was carried out by varying the ambient temperature with the remaining three parameters, see Figure 3. For this, the hidden variables were fixed to 20 °C for the dry-bulb temperature, 1 $^m/_s$ for the wind velocity and 50 % for the relative humidity. The code was adapted from [13]. Further, we ran a global, variance-based Sobol sensitivity analysis. It is a method that decomposes the variance in the UTCI into fractions which can be attributed to the four input variables. Generally, it is used to derive the rank-order importance of input variables in multivariate analyses. Beyond that, it is also helpful in not only gaining an understanding of how the variables affect the solution in sets of two but allow us to quantify the total effect when varying all parameters simultaneously (which cannot be plotted in two dimensions). The Saltelli implementation in SALib [9] was used to evaluate 100'000 samples of the UTCI problem space with the upper and lower bounds from Table 1. The upper and lower bounds were derived from the Syracuse weather data, except for the MRT, which has been assumed to be within a ±5 C° offset from the dry-bulb temperature.

Table 1. Variables and bounds for the global sensitivity analysis from the Syracuse weather data.

Variable	Unit	Min	Max
AmbTemp	$[^\circ C]$	-19.4	37.8
MRT	$[^\circ C]$	-24.4	42.8
Wind	$[^m/_s]$	0	17
RelHum	[%]	0	100

The aforementioned methods provide a good starting point to understand the dominance of the input variables in a theoretical framework. However, as cities shape their microclimates, they also shape the upper and lower bounds of the UTCI input variables in time and space. In this regard, the wind velocity and the MRT can be especially spatially-inhomogeneous due to wind sheltering effects or extreme surface temperatures. Therefore, we conducted a spatially-resolved global sensitivity analysis, for which the annual upper and lower bounds for each probing point serve as an input. For this, we probed the wind velocity and the MRT from the outdoor thermal comfort simulation results and made use of the weather data for ambient temperature and relative humidity.

2.4 Annual outdoor thermal comfort simulation framework

The simulation framework consists of two simulation engines, namely: OpenFOAM and Radiance. Both engines are centered around a toolkit called Eddy3D[2] that is implemented in Rhinoceros and Grasshopper which handles pre-, post-processing and the data handling between the simulation engines. Specifically, Eddy3D creates the simulation domain, specifies the boundary conditions, and takes care of processing the weather data based on the building geometry in Rhinoceros. Similarly, it uses Rhinoceros' meshing capabilities to export

[2] www.eddy3d.com

building meshes for both OpenFOAM and Radiance. Further, it uses Radiance to calculate irradiation and view factors for each sensor point.

Wind velocity

Due to the computationally-expensive nature of Computational Fluid Dynamics (CFD) simulations, it is infeasible to run a single analysis for an entire year. Considering this, we made use of the wind reduction factors method which has been implemented in Eddy3D. The tool utilizes OpenFOAM's $blockMesh$ utility for the background mesh and $snappyHexMesh$ to subsequently snap the background mesh to the building geometry. For the background mesh, we used a cylindrical simulation domain approach which allows reusing the same computational mesh for every wind direction, thus reducing the computation time and storage space [11]. Within the cylindrical mesh, we further refined the mesh within a refinement box that surrounds the buildings of interest. The simulation domain was set up according to best practices while taking into account all relevant surrounding buildings which resulted in $6.6 \cdot 10^6$ cells for the global mesh. This methodology makes use of a set of CFD simulations from several wind directions. For this study, we used 8 RANS simulations (0°, 45°, 90°, 135°, 180°, 225°, 270°, 315°) in a 45° interval. Depending on the direction, we mapped the inlets on the one-half circle of the simulation domain and the outlet on the opposite side. We used an incompressible, isothermal, steady-state solver from OpenFOAM in combination with a $k-\omega-SST$ turbulence model. The half-circular domain inlet was set to an atmospheric boundary layer (ABL) profile for U, k, and ω, and a roughness length $z_0 = 1$ that corresponds to a suburban environment. At the outlet of the computational domain, constant pressure is assumed, while the other variables are imposed to be zero-gradient. The ground and the building geometry used the same boundary conditions, a no-slip condition for velocity, a zero-gradient condition for the pressure and wall functions for U, k, and ω. Going forward, the 8 RANS simulations served as a nearest neighbor lookup table of wind velocities in concert with the annual weather data. For each probing point, we probed the simulated velocity from the 8 CFD simulations. This multidimensional array is used to calculate the dimensionless wind velocity for every probing point by dividing the simulated velocity magnitude by the scaled-down inlet velocity with the logarithmic wind power profile. This yields a spatial wind reduction matrix with information for every probing point for each of the 8 wind directions. From here, we converted the spatial matrix into a temporal matrix. For every hour of the year and its corresponding wind direction, we looked up the nearest neighbor CFD simulation and multiplied the velocities from the spatial velocity matrix with the wind velocity from the weather data that has been scaled down to the probing height. This operation yields a temporal velocity matrix with wind reduction data from which the wind velocities for the UTCI calculation are retrieved [10]. For cases where the wind velocity was outside the bounds of the UTCI calculation ($0.5\ ^m/_s <$ applicable range $< 17\ ^m/_s$), we replaced the values with lower and upper bounds and lifted the velocity at a height of 10 m as advised in [4].

Mean radiant temperature

The mean radiant temperature (MRT) calculated in this study consists of three components: the sky temperature T_{sky}, the solar gain (ΔMRT_{ds}) of being exposed to direct sun, and the ground and building surface temperature T_{gb}.

To estimate the ratio between T_{sky} and T_{gb}, we used Radiance to run a view factor analysis for every probing point. We calculated T_{sky} through the sky emissivity and the horizontal infrared radiation intensity [7]. We approximated T_{gb} with the ambient temperature as it has been shown that typical differences are less than $\pm 5\ K$ [12]. The solar gain to the human body is calculated using the Effective Radiant Field (ERF) [1] which we adapted for an outdoor setting and from which we derived (ΔMRT_{ds}). For the irradiance that is used as an input for the ERF, we implemented a Radiance-based Two-Phase (DDS) method. The DDS approach was chosen because it provides a better spatial resolution of the direct component. The Two-Phase DDS method is a daylight-coefficient-based simulation with an all-weather dynamic sky model (Perez Sky model). Instead of approximating the position and shape of the sun with few sky patches, we used 577 sun patches for the direct and diffuse simulation and 2305 direct sun patches. The illuminance is a linear combination of: (1) an annual daylight coefficient simulation, (2) annual direct-only daylight coefficients, and (3) an annual sun-coefficients simulation [3]:

$$E = C_{dc} \cdot S - C_{dcd} \cdot S_d + Csun \cdot S_{sun} \tag{2}$$

where C_{dc} and S denote the daylight coefficient matrix and the sky vector, C_{dcd} and S_d denote the direct-sky coefficient and the direct sky matrix, and C_{sun} and S_{sun} denote the direct-sun coefficient and the sun matrix, respectively. [16]. Finally, we computed the MRT for every hour h and every probe i according to Equation (3).

$$MRT_{h,i} = T_{sky,h} \cdot f_{sky,i} + T_{gb,h} \cdot f_{sky,i} + \Delta MRT_{ds,h} \tag{3}$$

2.5 Space usage

We used the data collected by Reinhart et al. [15] to estimate space usage around the Cornell University Engineering Quad to provide a meaningful metric for campus decision-makers. For this, we calculated the number of people for each hour and probing point as a function of the UTCI. The space usage is calculated for the three seasons spring, summer, and fall for occupancy periods between 10 am - 7 pm. All values were then normalized between 0 - 1 as the empirical data cannot be directly applied to a different university campus without further investigation.

3 RESULTS

Both non-spatial sensitivity analyses justify the assumptions that have been made when setting up the simulation framework.

Two-at-a-time sensitivity analysis

In Figure 3, each input variable to the UTCI metric shows a non-linear behavior when varying it with the ambient temperature, however, their amplitude and parameter range differ

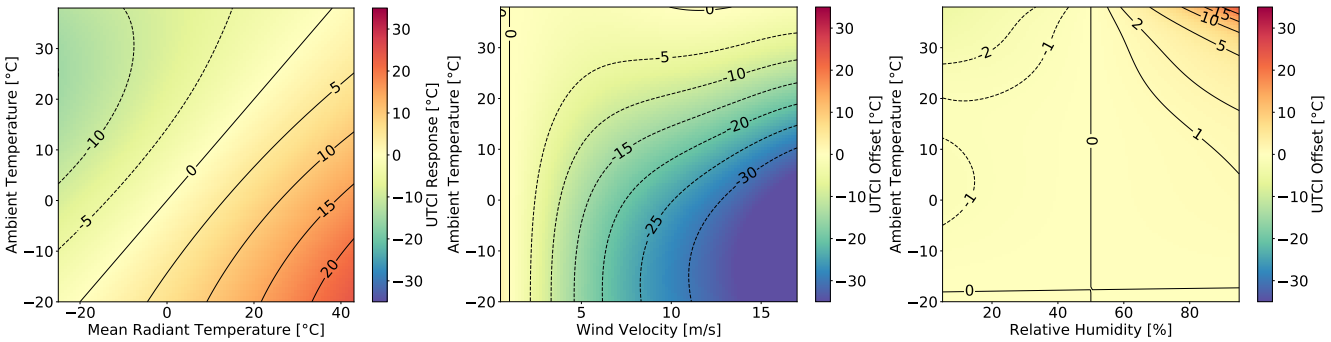

Figure 3. Two-at-a-time sensitivity analysis of the UTCI input variables.

significantly. When varying the MRT with the ambient temperature in Figure 3 (a), high and low MRTs create significant discomfort through temperature asymmetry. For the wind velocity in Figure 3 (b), we see highly non-linear behavior for both low ambient temperatures and high wind velocities. This effect is commonly known as the wind chill due to increased forced convection. When varying the ambient temperature with relative humidity, non-linear behavior is evident only for high levels of both relative humidity and ambient temperature.

Global sensitivity analysis

Figure 4 quantifies the first-, second-, and total-order sensitivity indices illustrated as black dots, gray lines, and black circles, respectively. The confidence intervals for each index and variable were found to be below $1 \cdot 10^{-2}$. We confirm that the dominant variables contributing to the UTCI in a climate in upstate NY were ambient temperature, MRT, and wind velocity. Those three variables show total-order sensitivity indices of 83 %, 5 %, 16 %, respectively. The least dominant factor in this climate is the relative humidity which only accounts for 1 % of the variance. This suggests that the humidity may be neglected for the Dfb climate zone. Note that the total sensitivity indices sum to a value greater than one, indicating that the input variables are to some extent correlated. The second-order sensitivity indices range from ~1 - 5 % with wind and ambient temperature showing the largest interaction effects. This confirms the findings from the two-at-a-time sensitivity analysis, see Figure 3 (b).

Annual outdoor thermal comfort

All results in this section have been computed and probed at a height of 2 m above ground. Figure 5 (a) shows the averaged annual wind velocity magnitudes. We see that points that are sheltered from the wind experience a lower pedestrian comfort rating and vice versa. It is also evident that venturi effects exist in two areas, channeling the wind from north to south. Figure 5 (b) shows the averaged annual mean radiant temperature. The average MRT ranges from 4.5-6.5°C where higher temperatures are seen closed to building geometries and vice versa. Figure 5 (c) shows the averaged annual UTCI. While points close to building geometries generally see favorable conditions in terms of wind velocities and MRTs, it is evident that the venturi effect sports are rendered less comfortable. Overall, the seating arrangements on the Engineering Quad are within areas that show a rather high annual averaged UTCI.

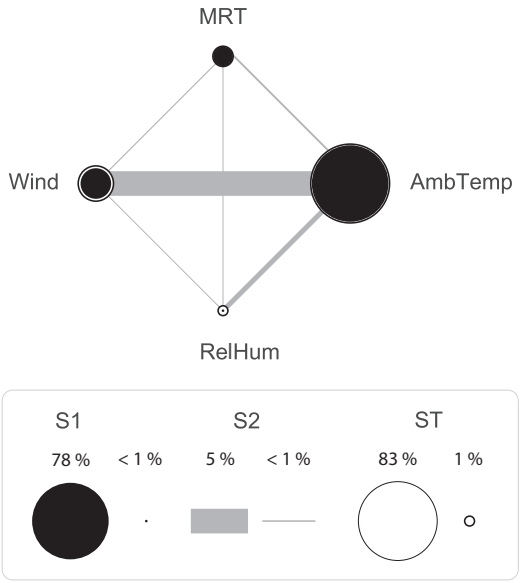

Figure 4. Global sensitivity indices where S1 is the first-order, S2 is the second-order, and ST is the total-order effect for the UTCI estimated with the Sobol method.

Space usage

In Figure 5 (d) we show the predicted space usage around the campus on June 30, 16:00 h, a hot and calm day from the weather file for which the average UTCI was estimated to 33°C. We focus on hourly data in this part of the results as an annual average would not allow to highlight the temporal variance and its effect on space usage. Areas with exposure to direct sun receive a penalty in terms of space usage due to wind not being present. By contrast, shaded areas experience increased numbers of space usage as those are the only ones with a comfortable UTCI. Here, the seating arrangements on the Engineering Quad suffer from direct exposure to sunlight. Given the already uncomfortable conditions (UTCI = 33°C), the seating arrangements and other areas exposed to direct sunlight suffer a penalty.

Spatially-resolved global sensitivity analysis

Figure 6 (a) and Figure 6 (b) show the spatially-resolved total sensitivity indices for the wind velocity and the MRT. The upper bound for ST for the wind velocity is close to 40 %,

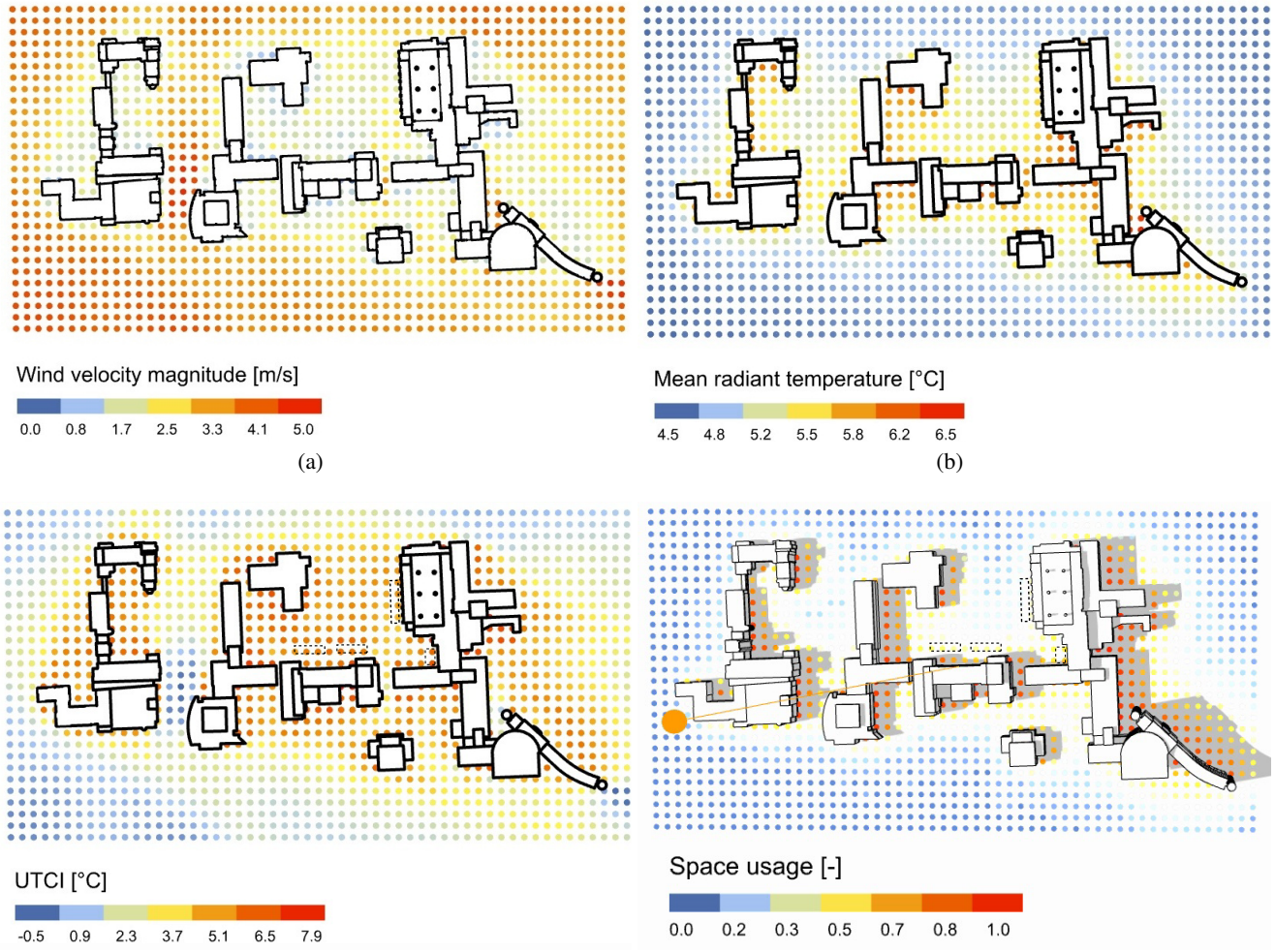

Figure 5. (a) Annual wind velocity magnitudes; (b) average annual mean radiant temperature; (c) average annual UTCI; (d) estimated space usage on June 30, 16:00 h, a hot and calm day from the weather file. The dashed markers indicate actual outdoor seating arrangements on campus.

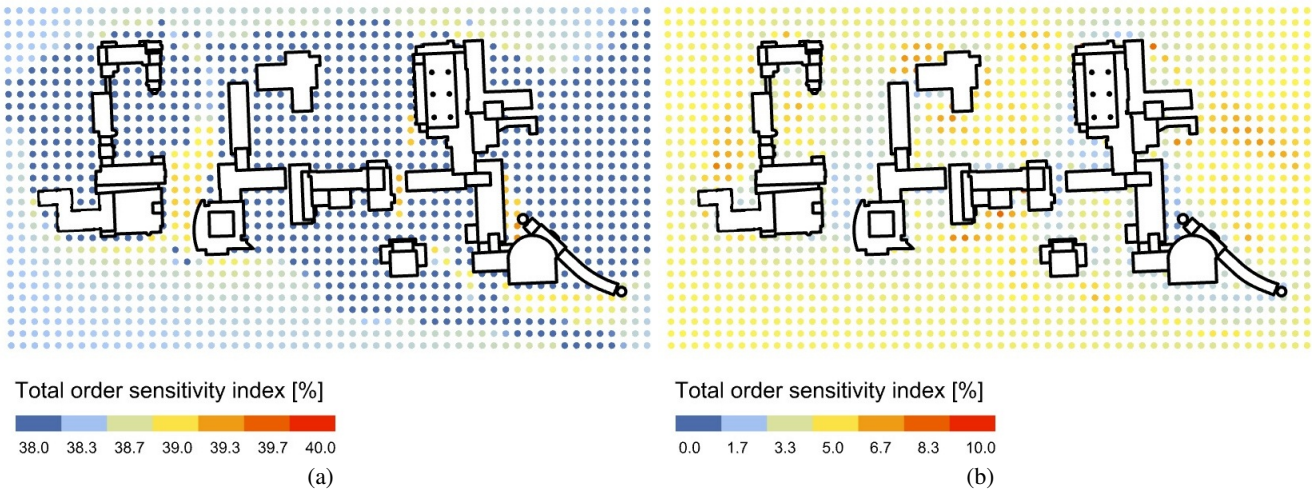

Figure 6. Spatially-resolved total sensitivity index for the (a) the wind velocity and (b) the mean radiant temperature.

whereas the upper bound for the MRT is around 10 %. For example, the wind velocity around two north-south corridors in Figure 6 (a), explains a large part (~40 %) of the variance in the UTCI output considering an entire year.

4 DISCUSSION

We used weather data from Syracuse, NY as boundary conditions for this study as there is limited data available for the site in Ithaca, NY. While ambient temperature and irradiation of both sites are comparable, it is conceivable that Ithaca, NY experiences deviating wind velocity distributions due to its overall differences in elevation and its location at the edge of a valley. Further, using empirical data from another university campus in Boston to estimate space usage has limitations. Despite the overall climate in Boston being similar, it lies in a different sub-climate zone with hotter summers than those in upstate NY. Although Reinhardt et al. [15] suggest their results hold for climate comparable to Boston's, the relationship between UTCI and space usage in upstate NY be likely different. Nonetheless, in this study, we argue for the importance of decision aiding based on outdoor thermal comfort results rather than their validation.

We have shown that local, global, and spatially-global sensitivity analyses can help understand the dominant input variables of a complex metric such as the UTCI. The results of the global sensitivity analysis in Figure 4 reveal the strong second-order interaction between the ambient temperature and the wind velocity. That is to say that, without plotting the relationship between both variables, we know that a large part of the variance in the UTCI can be attributed to varying both the ambient temperature and the wind velocity simultaneously. It is worth noting that the global analysis itself does not reveal the inverse nature of this relationship (an increase in wind velocity and a decrease in dry-bulb temperature yields a non-linear decrease in UTCI). As sensitivity analyses help assess arbitrary functions (such as the UTCI), generalizing this insight might be helpful for practitioners in the design process. In that regard, we suggest to use a global sensitivity analysis as a first step when analyzing a (potentially unknown) metric, and to derive a factor prioritization from it. Identifying second-order effects (gray lines in Figure 4) will help to determine which "slices" of the solution space to plot in two dimensions to better understand the relationship of the variables.

The 16 % total sensitivity of the wind velocity warrants a discussion of the limitation of the annual wind velocity method, see Figure 5 (a). First, the number of wind directions simulated determines the accuracy of the result, although, the increase shows diminishing returns. Although the authors are aware that a higher number of wind directions will increase the overall accuracy of the annual wind velocity magnitudes, we refrained from simulating additional wind direction in the interest of time. Further, for each of the 8 simulations, a constant inlet wind velocity of 5 $^{m}/_{s}$ at 10 m was assumed, regardless of the distribution of wind directions and their corresponding hourly wind velocities. This was justified by Becker et al. [2] that have shown that the reattachment length behind a cube does not change significantly for Reynolds numbers greater than $1 \cdot 10^5$ which applies for this study. In general, however, the wind velocities between the buildings on campus are likely overestimated as not all surrounding buildings on campus have been included in the CFD simulation.

The range of the averaged annual MRT in Figure 5 (b) seems reasonable as the average dry-bulb temperature is 10 °C. A closer inspection of the annual MRT time series revealed that the shaded MRT is generally very close to the dry-bulb temperature, whereas the nighttime MRT lies ~10°C below. This confirms the findings by [12]. The current simulation framework, however, does not take into account radiative heat exchange and therefore does not take into account urban heat islands that are likely to occur during summer. Although Kessling et al. [12] argue that the difference between surface and dry-bulb temperatures usually below ±5 K even in very hot climates, it is not clear if those findings are generalizable for arbitrary building densities, other than Riyadh. Here, more research is required to establish a more holistic and robust workflow.

It is worth noting that the ranges for the spatially-resolved sensitivity analysis in Figure 6 (a) and Figure 6 (b) differ from those in Figure 4. That is to say that locally, the bounds for each point differ significantly from the assumptions made in Table 1. Moreover, the areas with high total-order sensitivity indices in Figure 6 (a) and Figure 6 (b) confirm what was expected by the average annual UTCI distribution. The areas colored in red may be interpreted as the areas for which the respective variable (wind velocity / MRT) is controlling most of the variance in the UTCI output. For example, in areas where the wind velocity is high on average (north-south corridors), the wind velocity is relatively dominant. Besides, Figure 6 (b) suggests that wind shelters might be beneficial to improve the annual outdoor comfort for the seating arrangements to the west of the building as the MRT variance in the output is relatively low. Insights from such visualizations will prove to be helpful in other studies when decision-makers decide about possible interventions to promote good outdoor thermal comfort.

Future studies should combine spatial and temporal sensitivity studies. A preliminary sensitivity analysis of the UTCI for different climate zones has shown that the complexity of outdoor comfort metrics typically causes a subset of parameters to be inactive at any particular time; and that the inactive input variables differ from climate zone to climate zone. This sparsity of activation may lead to needless computational complexity and inappropriate assumptions of parameters that are inactive in the first place. Combining spatial and temporal sensitivity analyses (ideally by season) might present a valuable opportunity to overcome the complexity of simulation engines. In effect, this would be achieved by restricting the variable input space to only those parameters which are actively contributing to the output at a specific time and location for the particular climate zone.

5 CONCLUSIONS

Exploring parameter activation at the spatial and temporal scales is important not only for diagnostic analyses of biometeorological indices such as the UTCI but also to provide

actionable insights when deciding about potential interventions. This study represents a novel step in this direction by visualizing the spatial sensitivity of the UTCI and exemplifies how to derive the outdoor space usage as a proxy for the attractiveness of outdoor spaces. We conclude that the spatial variability of any outdoor comfort metric can easily be visualized which provides valuable information about its behavior. As the availability of computing power continues to increase, we anticipate the community to look beyond results only; instead, we anticipate using them to derive actionable insights which to date remained largely unexplored.

REFERENCES

1. Arens, E., Hoyt, T., Zhou, X., Huang, L., Zhang, H., and Schiavon, S. Modeling the comfort effects of short-wave solar radiation indoors. *Building and Environment 88* (2015), 3–9.
2. Becker, S., Lienhart, H., and Durst, F. Flow around three-dimensional obstacles in boundary layers. *Journal of Wind Engineering and Industrial Aerodynamics 90*, 4-5 (2002), 265–279.
3. Bourgeois, D., Reinhart, C. F., and Ward, G. Standard daylight coefficient model for dynamic daylighting simulations. *Building Research & Information 36*, 1 (2008), 68–82.
4. Bröde, P., Fiala, D., Błażejczyk, K., Holmér, I., Jendritzky, G., Kampmann, B., Tinz, B., and Havenith, G. Deriving the operational procedure for the universal thermal climate index (utci). *International journal of biometeorology 56*, 3 (2012), 481–494.
5. Broede, P., Blazejczyk, K., Fiala, D., Havenith, G., Holmer, I., Jendritzky, G., Kuklane, K., and Kampmann, B. The universal thermal climate index utci compared to ergonomics standards for assessing the thermal environment. *Industrial health 51*, 1 (2013), 16–24.
6. Bui, Q., and White, J. Mapping the shadows of new york city: Every building every block. *New York Times* (2016).
7. EnergyPlus Documentation. Engineering Reference - EnergyPlus 8.9. *The Reference to EnergyPlus Calculation* (2019).
8. Fiala, D., Havenith, G., Bröde, P., Kampmann, B., and Jendritzky, G. Utci-fiala multi-node model of human heat transfer and temperature regulation. *International journal of biometeorology 56*, 3 (2012), 429–441.
9. Herman, J., and Usher, W. Salib: an open-source python library for sensitivity analysis. *Journal of Open Source Software 2*, 9 (2017), 97.
10. Kastner, P., and Dogan, T. Towards high-resolution annual outdoor thermal comfort mapping in urban design. In *Proceedings of Building Simulation 2019: 16th Conference of IBPSA* (2019).
11. Kastner, P., and Dogan, T. A cylindrical meshing methodology for annual urban computational fluid dynamics simulations. *Journal of Building Performance Simulation 13*, 1 (2020), 59–68.
12. KESSLING, W., ENGELHARDT, M., and KIEHLMANN, D. The human bio-meteorological chart. In *PLEA* (2013).
13. Kongsgaard, C. Utci parameter sensitivity, 2012.
14. Provençal, S., Bergeron, O., Leduc, R., and Barrette, N. Thermal comfort in quebec city, canada: sensitivity analysis of the utci and other popular thermal comfort indices in a mid-latitude continental city. *International journal of biometeorology 60*, 4 (2016), 591–603.
15. Reinhart, C. F., Dhariwal, J., and Gero, K. Biometeorological indices explain outside dwelling patterns based on wi-fi data in support of sustainable urban planning. *Building and Environment 126* (2017), 422–430.
16. Subramaniam, S. Daylighting simulations with radiance using matrix-based methods. *Lawrence Berke-ley National Laboratory* (2017).
17. Tumini, I., and Rubio-Bellido, C. Measuring climate change impact on urban microclimate: A case study of concepción. *Procedia engineering 161* (2016), 2290–2296.
18. Whyte, W. H. *City: Rediscovering the center*. University of Pennsylvania Press, 2012.
19. Whyte, W. H., et al. *The social life of small urban spaces*. Conservation Foundation Washington, DC, 1980.